

# The freeze-out properties of hyperons in a microscopic transport model

Zhenglian Xie<sup>1,2</sup>, Pingzhi Ning<sup>1</sup> and Steffen A. Bass<sup>2</sup>

<sup>1</sup> School of Physics, Nankai University, Tianjin 300071, China

<sup>2</sup> Department of Physics, Duke University, Durham, North Carolina 27708-0305, USA

E-mail: xiezhenglian@mail.nankai.edu.cn

**Abstract.** The excitation function of freeze-out time, average freeze-out temperature and freeze-out energy density of (multi-) strange baryons created in relativistic heavy-ion collisions is investigated in the framework of a microscopic transport model. We find that the  $\Omega$  on average freezes out earlier than the nucleon,  $\Lambda$  and  $\Xi$ . The average freeze-out temperature and energy density as well as the spread between the different baryonic states increase monotonously with increasing beam energy and should approach a universal value in the case of a hadronizing Quark-Gluon-Plasma.

Submitted to: *J. Phys. G: Nucl. Phys.*

## 1. Introduction

A major goal of colliding heavy-ions at relativistic energies is to heat up a small region of space-time to temperatures as high as are thought to have occurred during the early evolution of the universe, a few microseconds after the big bang [1]. In ultra-relativistic heavy-ion collisions, such as are currently being explored at the Relativistic Heavy-Ion Collider (RHIC), the four-volume of hot and dense matter, with temperatures above  $\sim 150$  MeV, is on the order of  $\sim (10 \text{ fm})^4$ . The state of strongly interacting matter at such high temperatures (or density of quanta) is usually called quark-gluon plasma (QGP) [2, 3].

The first five years of RHIC operations at  $\sqrt{s_{NN}} = 130$  GeV and  $\sqrt{s_{NN}} = 200$  GeV have yielded a vast amount of interesting and sometimes surprising results [4, 5, 6, 7], many of which have not yet been fully evaluated or understood by theory. There exists mounting evidence that RHIC has created a hot and dense state of deconfined QCD matter with properties similar to that of an ideal fluid [8, 9] – this state of matter has been termed the *strongly interacting Quark-Gluon-Plasma* (sQGP).

The central problem in the study of the sQGP is that the deconfined quanta of a sQGP are not directly observable due to the fundamental confining property of the physical QCD vacuum. If we could see free quarks and gluons (as in ordinary plasmas) it would be trivial to verify the QCD prediction of the QGP state. However, nature chooses to hide those constituents within the confines of color neutral composite many body systems – hadrons. One of the main tasks in relativistic heavy-ion research is to find clear and unambiguous connections between the transient (partonic) plasma state and the observable hadronic final state (for reviews on QGP signatures, please see [10, 11]). Among the currently pressing issues in the exploration of the (s)QGP is the question at temperature and energy-density deconfinement is achieved. In order to address this question, a low energy run is being performed at RHIC and the new FAIR project at GSI is aiming in the same direction. What is now needed most is a set of robust signatures which could indicate the transition from an excited hadron gas to a deconfined state of (strongly interacting) quarks and gluons.

The investigation of strangeness production in relativistic heavy ion collisions has been proven to be a powerful tool for the study of highly excited nuclear matter, both in terms of the reaction dynamics and in terms of its hadrochemistry [12, 13, 14, 15, 16, 17, 18, 19, 20, 21]. Furthermore, strangeness has been suggested as a signature for the creation of a Quark-Gluon-Plasma (QGP) [12, 13, 14]: in the final state of a heavy-ion collision, subsequent to the formation and decay of a QGP, strangeness has been predicted to be enhanced relative to the strangeness yield in elementary hadron+hadron collisions.

The slope parameters of (multi-)strange baryons transverse momentum distributions have been measured at the CERN SPS [22, 23, 24] and at RHIC [25, 26]. They exhibit a characteristic deviation from a hydrodynamically motivated blastwave expansion [27]. This *reduction* in the slope parameter has been shown in microscopic and

hybrid macro+micro transport models to be caused early freeze-out of (multi-)strange baryons due to their reduced hadronic cross sections, compared to non-strange baryons [27, 28, 29, 30]. It is the purpose of our analysis to explore whether this feature is prevalent at lower beam energies as well and whether it can possibly be exploited as an indicator for the transition from an excited hadron gas to a (s)QGP.

## 2. The UrQMD model

For our studies we use the Ultra-relativistic Quantum Molecular Dynamics (UrQMD) model, a microscopic hadronic transport model with hadron and constituent (di-)quark degrees of freedom. In UrQMD system evolves as a sequence of binary collisions or 2 –  $N$ -body decays of mesons, baryons, and constituent (di-)quarks. Binary collisions are performed in a point-particle sense: Two particles collide if their minimum distance  $d$ , i.e. the minimum relative distance of the centroids of the Gaussians during their motion, in their CM frame fulfills the requirement:

$$d \leq d_0 = \sqrt{\frac{\sigma_{\text{tot}}}{\pi}}, \quad \sigma_{\text{tot}} = \sigma(\sqrt{s}, \text{ type}). \quad (1)$$

The cross section is assumed to be the free cross section of the regarded collision type ( $N - N$ ,  $N - \Delta$ ,  $\pi - N \dots$ ).

Especially when studying the hadrochemistry of a heavy-ion reaction it is of great importance to include as many hadronic states as possible into the model calculation: The UrQMD collision term contains 49 different baryon species (including nucleon, delta and hyperon resonances with masses up to 2 GeV) and 25 different meson species (including strange meson resonances), which are supplemented by their corresponding anti-particle and all isospin-projected states. Full baryon/antibaryon symmetry is included. For excitations with higher masses a string picture is used. All states listed can be produced in string decays, s-channel collisions or resonance decays.

Tabulated or parameterized experimental cross sections are used when available, resonance absorption and scattering is handled via the principle of detailed balance. If no experimental information is available, the cross section is either calculated via an OBE model or via a modified additive quark model which takes basic phase space properties into account. A detailed overview of the elementary cross sections and string excitation scheme included in the UrQMD model is given elsewhere [31, 32].

## 3. Strangeness production in UrQMD

Strangeness may be produced either in initial collisions among the incoming nucleons of the two colliding nuclei or through secondary interactions among produced particles, e.g. pions and nucleons or excited resonances.

For collision energies which lead to the creation of a hadron gas at temperatures up to approx. 140 MeV, the dominant strangeness production mechanism in UrQMD utilizes a resonance gas approach: here strangeness production is a two step process.

Initially a heavy baryon resonance is excited, e.g. via  $p + p \rightarrow N + N_{1710}^*$ , which subsequently decays via  $N_{1710}^* \rightarrow Y + K^+$ . Subsequently, the hyperon could rescatter with a kaon to form a  $\Xi^*$  resonance, which could decay into a  $\Xi + \pi$  final state to facilitate  $\Xi$  production. This approach allows for an easy extension into the higher energy domain and may provide some rudimentary guidance for unknown strangeness production cross sections in secondary collisions, e.g.  $\pi + N \rightarrow N_{1710}^* \rightarrow Y + K^+$ . The aforementioned secondary interactions like pion-induced strangeness production or flavor-exchange reactions are at least as important for the reaction dynamics and final strangeness yield as the initial/primordial strangeness production channels. The hyperon resonances which are excited via this cross section may either decay again into the  $K^- + N$  channel, or to almost equal probability decay into the  $Y + \pi$  channel, thus transferring strangeness in and out of baryonic degrees of freedom. At beam energies in the SIS and low AGS domain this  $K^- + N \leftrightarrow Y + \pi$  exchange reaction is of particular importance.

At higher incident beam energies, particle production in general is dominated by string excitation and fragmentation. Up to 70% of the total strangeness produced in a Pb+Pb collision at top CERN-SPS energies is produced in initial highly energetic nucleon-nucleon interactions which lead to the excitation and subsequent fragmentation of strings. On an elementary hadron-hadron level, the parameters of the string fragmentation are fitted to measured multiplicities and momentum distributions.

For our analysis we have calculated and analyzed the time-evolution of central Au+Au collisions at 10.6, 20, 40, 80 and 160 GeV/nucleon. Typically we have calculated between 15K and 50K collisions per incident beam energy. Figure 1 shows the transverse momentum spectra of baryons produced in central Au+Au collisions at 20, 80 and 160 GeV/nucleon incident beam energy and serves as a model baseline which can directly be compared to the final state accessible by the experiments.

#### 4. Methodology: freeze-out times, temperatures and energy-densities

In this section we shall discuss the basic concepts which enter into our analysis: the main task is to calculate the local temperature and local energy-density a baryon experiences at any given time during the collision evolution. We accomplish this by transforming the momenta of all particles in the system into the local rest-frame of the respective baryon, calculating the kinetic energy of all surrounding hadrons within a radius of 1 fm, and then utilizing the equipartition theorem to determine the local temperature. The local energy density is trivially calculated by summing over the total energy of all hadrons in the sphere and dividing by the volume of that sphere. The radius of the sphere has been chosen such that it contains a sufficient number hadrons for the temperature and energy-density extraction, but is still sufficiently small to provide a local measure of temperature and energy-density.

The freeze-out time and position of a hadron is defined to be the location and time of its last interaction, i.e. scattering. While the concept of a freeze-out time is

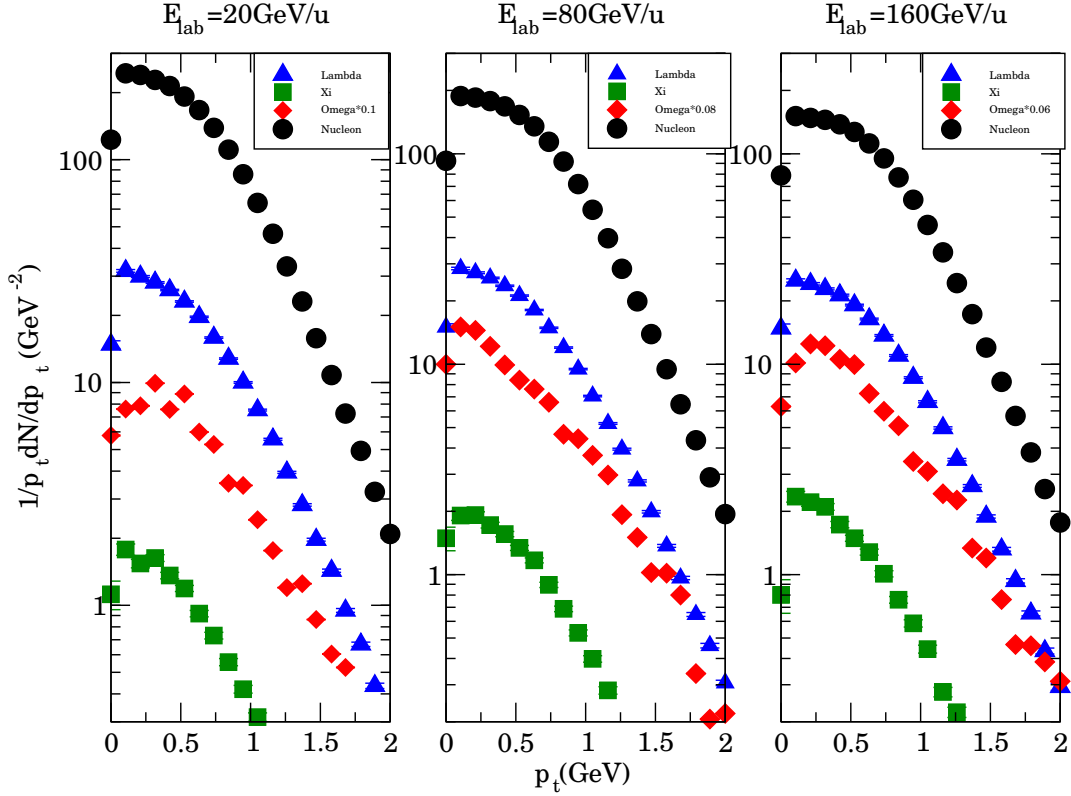


**Figure 1.** Transverse momentum spectra of baryons produced in central Au+Au collisions at mid-rapidity and 20, 80 and 160 GeV/nucleon incident beam energy.

thus well-defined on the basis of an individual hadron, it is less well-defined for a given particle species or even the full system as a whole. Referring to a specific freeze-out time (or temperature) of a hadron species, or even the entire collision system, is only an approximation, which at most can hold true on average. Figure 2 shows the distribution of freeze-out times at mid-rapidity for the different baryon species in Au+Au collisions at incident beam energies of 20 GeV/nucleon (left) and 160 GeV/nucleon (right). The normalization is chosen such that all curves integrate to unity in order to facilitate the comparison between the different hadron species.

As one can see in Figure 2, the freeze-out distributions for all baryons are very broad - basically baryons are ejected from the reaction zone continuously over the entire time-evolution of the reaction. Nevertheless, some interesting trends are visible, most notably the freeze-out time distribution of the Omega is peaked significantly earlier than that of the other baryons. We would expect the  $\Xi$  to show a similar trend as the  $\Omega$ , but suffer from contamination due to the long life-time (i.e. narrow decay width) of the  $\Xi^*(1530)$  resonance, which is responsible for the long tail towards late times in the freeze-out time distribution of the  $\Xi$ . In order to facilitate our analysis of the Au+Au energy excitation function, we need to condense the information present in these freeze-out time distributions by averaging over these distributions. This can be done in several ways:

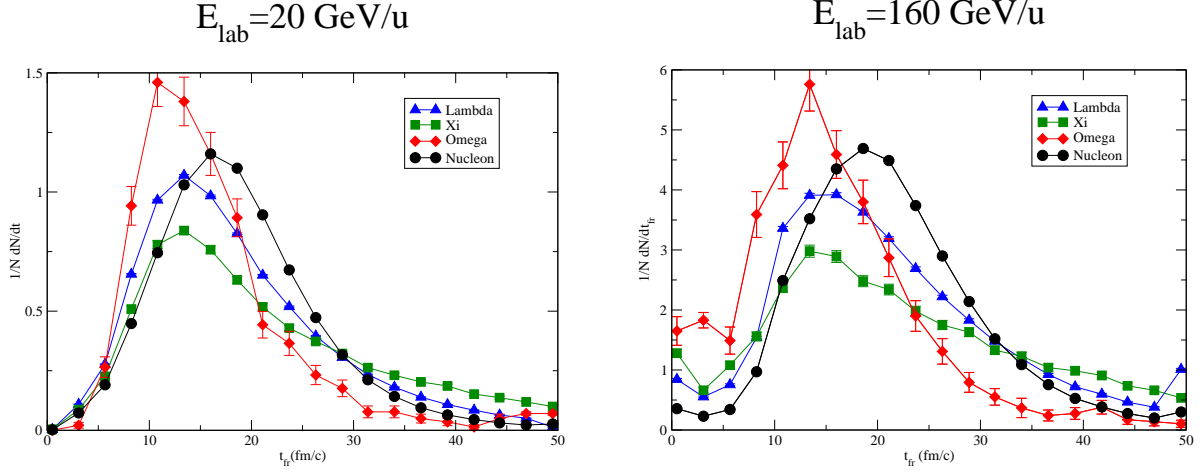


**Figure 2.** Normalized freeze-out time distributions for nucleons , Lambda's, Xi's and Omega's in Au+Au collisions at  $E_{lab}=20\text{GeV/u}$  (left) and  $E_{lab}=160\text{ GeV/u}$  (right).

**Table 1.** The calculated freeze-out time of N,  $\Lambda$ ,  $\Xi$  and  $\Omega$ .

| Energy(Gev/u) | N(fm/c) | $\Lambda$ (fm/c) | $\Xi$ (fm/c) | $\Omega$ (fm/c) |
|---------------|---------|------------------|--------------|-----------------|
| 10.6          | 18.8    | 18.9             | 24.1         | 16.7            |
| 20.0          | 18.8    | 18.9             | 24.6         | 16.1            |
| 40.0          | 19.2    | 19.3             | 24.2         | 15.8            |
| 80.0          | 20.1    | 20.2             | 24.7         | 15.8            |
| 160.0         | 21.2    | 21.2             | 25.5         | 16.2            |

- the *average* freeze-out time  $\bar{t}_f$  of a species is being calculated by averaging the individual freeze-out times of all particles of that species – mathematically it constitutes the average of the distributions depicted in Figure 2. The shortcoming of this definition is that the distributions are rather broad and that a significant fraction of all particles of a given species may continue to interact well beyond that time.
- alternatively we can define the freeze-out time of a species to be at that instant when e.g. 80% of its particles have ceased interacting:  $t_f^{80\%}$ . The advantage of this definition lies in its better connection to the dynamics of the system, i.e. most particles of the species have frozen out at that time.

## 5. Results and discussion

Let us first investigate the connection between the different freeze-out time distributions of the final state baryon species (nucleon, hyperon, Cascade and Omega) and their average freeze-out temperature. We focus on baryons emitted within  $\pm 1$  unit around mid-rapidity. In Figure 3 we have calculated the average freeze-out temperature of the four final state baryon species as a function of time, i.e. at each time-step we have

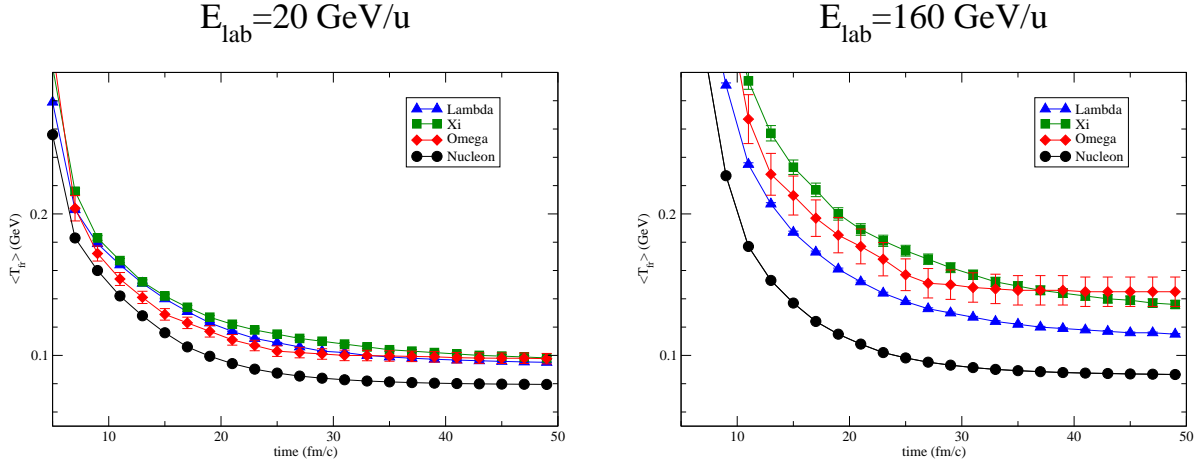


**Figure 3.** The average freeze-out temperature for Nucleons, Lambda's, Xi's and Omega's as function of time for  $E_{lab}=20\text{ GeV/u}$  (left) and  $E_{lab}=160\text{ GeV/u}$  (right). A saturation of the respective curve indicates that the majority of particles of that species have ceased interacting.

calculated the average local temperature at the last previously encountered interaction point for all nucleons, hyperons, cascades and omegas in the system. A leveling off of that temperature signifies the freezing out of the majority of baryons of that species and in the long time limit these curves converge to the overall average freeze-out temperature for a given species. The left frame of Figure 3 shows our analysis for an incident beam energy of 20 GeV/nucleon and the right frame shows the same analysis for 160 GeV/nucleon. The final average freeze-out temperature for N,  $\Lambda$ ,  $\Xi$  and  $\Omega$  at  $E_{lab}=160\text{ GeV/nucleon}$  are 86.5, 115, 136 and 145 MeV respectively. A careful study of Figure 3 indicates at what time during the evolution of the reaction the freeze-out temperature 'saturates' and the respective baryon species thus becomes insensitive to the subsequent evolution of the system. Comparing the two incident beam energies, we find that there is very little difference in the freeze-out temperatures among (multi-)strange baryon species at 20 GeV/nucleon and that a more pronounced ordering according to strangeness content develops at the higher beam energy. In both cases the nucleons exhibit a significantly lower freeze-out temperature than strange baryons.

Figure 4 shows the same analysis as Figure 3, but for the freeze-out energy-density instead of the freeze-out temperature. It is interesting to note that whereas at 160 GeV/nucleon we observe exactly the same trends in terms of the freeze-out energy-density as we did for the freeze-out temperature, at 20 GeV/nucleon the  $\Omega$  seems to probe a higher freeze-out energy density than the  $\Xi$  and the hyperons, differing from our findings for the freeze-out temperature. At 160 GeV/nucleon we find the average freeze-out energy densities for N,  $\Lambda$ ,  $\Xi$  and  $\Omega$  to be 0.3, 0.57, 0.85 and 0.84  $\text{GeV}/(fm)^3$  respectively.

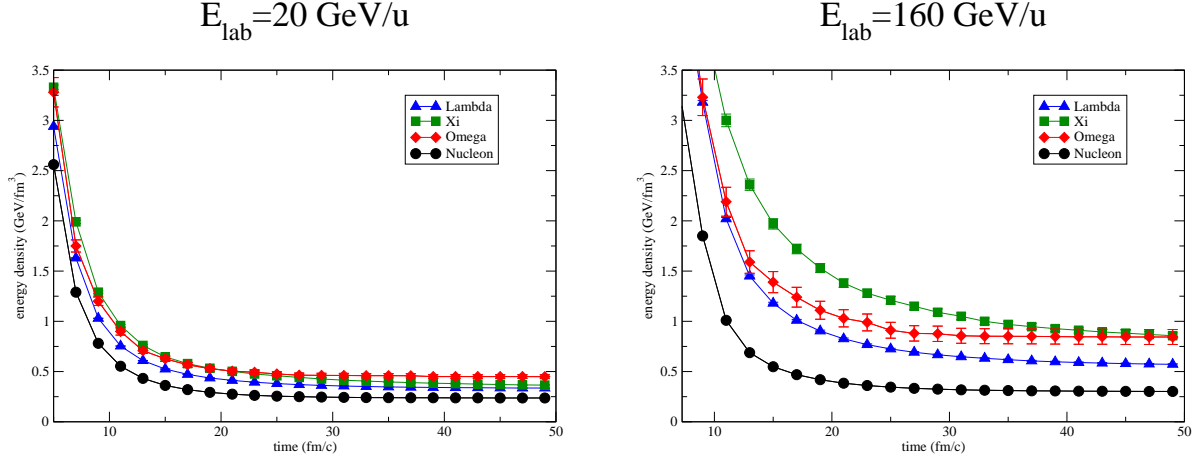


**Figure 4.** The average freeze-out energy density for Nucleons, Lambda's, Xi's and Omega's as a function of time for  $E_{lab}=20\text{GeV/u}$  (left) and  $E_{lab}=160\text{GeV/u}$  (right). A saturation of the respective curve indicates that the majority of particles of that species have ceased interacting.

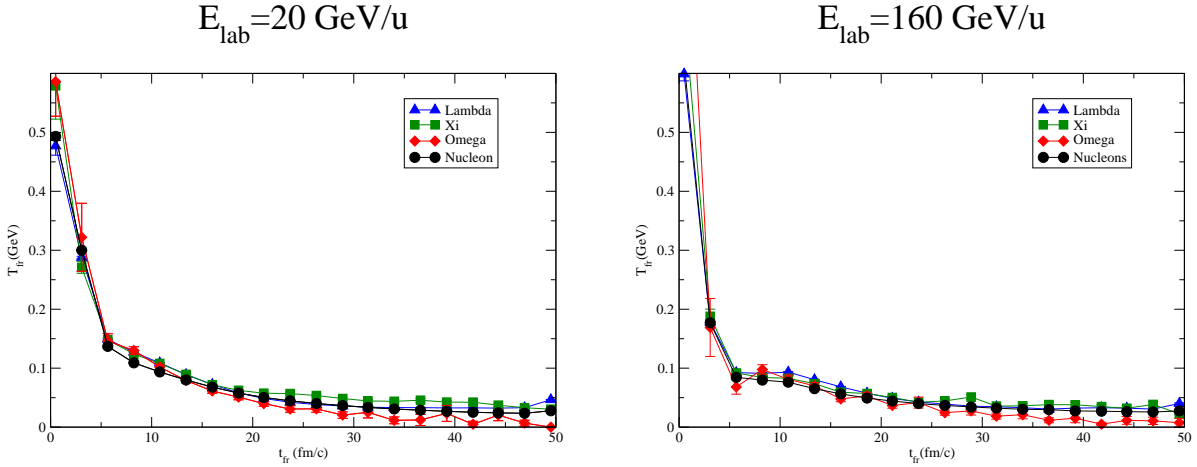


**Figure 5.** Freeze-out temperature as a function of freeze-out time for Nucleons, Lambda's, Xi's and Omega's for  $E_{lab}=20\text{GeV/u}$  (left) and  $E_{lab}=160\text{GeV/u}$  (right). The agreement between the curves indicates that baryons freezing out at identical times probe the same medium, irrespective of their species.

If the picture we have developed regarding the dynamics of hadron freeze-out and its flavor sensitivities is correct, then a nucleon and a  $\Omega$  baryon freezing out *at the same time* within similar conditions (i.e. mid-rapidity) should be probing the same medium in terms of its temperature and energy-density:

Figure 5 shows the average freeze-out temperature for all particles freezing out *at a given time*, i.e. for each time-step we evaluate the freeze-out temperature only for those baryons whose final interaction actually occurs in that timestep. The figures (left for 20 GeV/nucleon and right for 160 GeV/nucleon incident beam energy) confirm our hypothesis – all four baryon species exhibit near identical freeze-out temperatures for



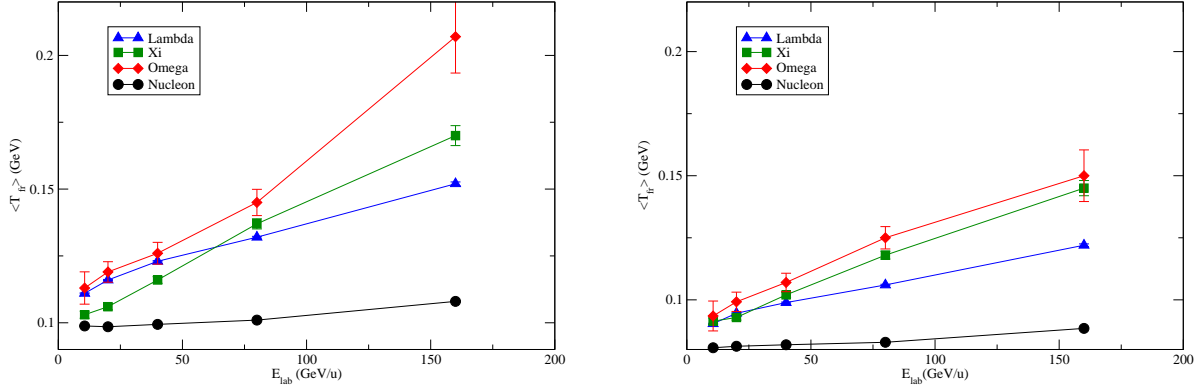


**Figure 6.** Average freeze-out temperature vs beam energy for final state baryons. The freeze-out temperature is calculated at the average freeze-out time (left) and at the time when 80 percent of Nucleons, Lambda, Xi and Omega have ceased interacting (right).

final interactions occurring at identical times.

Let us now investigate how our results depend on the incident beam energy of the heavy-ion collision: Figure 6 shows the excitation function of freeze-out temperatures for the four different baryon species vs. incident beam energy for central Au+Au collisions. The left frame displays the average freeze-out temperature at the average freeze-out time for each species, whereas the right frame takes the freeze-out temperature at the time when 80% of all particles of each species have ceased interacting. Naturally in the latter case we obtain somewhat lower freeze-out temperatures due to later freeze-out times (and thus lower freeze-out temperatures) contributing to the analysis. The only other quantitative difference between the two analyses is the  $\Xi$ , since for the average freeze-out time criterion we encounter contamination by the long-lived  $\Xi^*(1530)$  resonance, leading to a larger average freeze-out time for the  $\Xi$ .

Figure 7 shows the same analysis as Figure 6, but with the freeze-out energy-density instead of freeze-out temperature. It is interesting to note that for both quantities and the more realistic 80% criterion, at 160 GeV/nucleon incident beam energy the  $\Omega$  exhibits a freeze-out temperature and energy-density very close to the critical temperature and energy-density of the deconfinement phase transition.

## 6. Summary

We have calculated the excitation function of freeze-out time, average freeze-out temperature and freeze-out energy-density of final state baryons created in relativistic heavy-ion collisions within the UrQMD model. We find that the  $\Omega$  on average freezes out earlier than the nucleon,  $\Lambda$  and  $\Xi$  and thus exhibits a higher freeze-out temperature and energy-density. In general, baryons systematically freeze out earlier with rising strangeness content. The average freeze-out temperature and energy density as well as

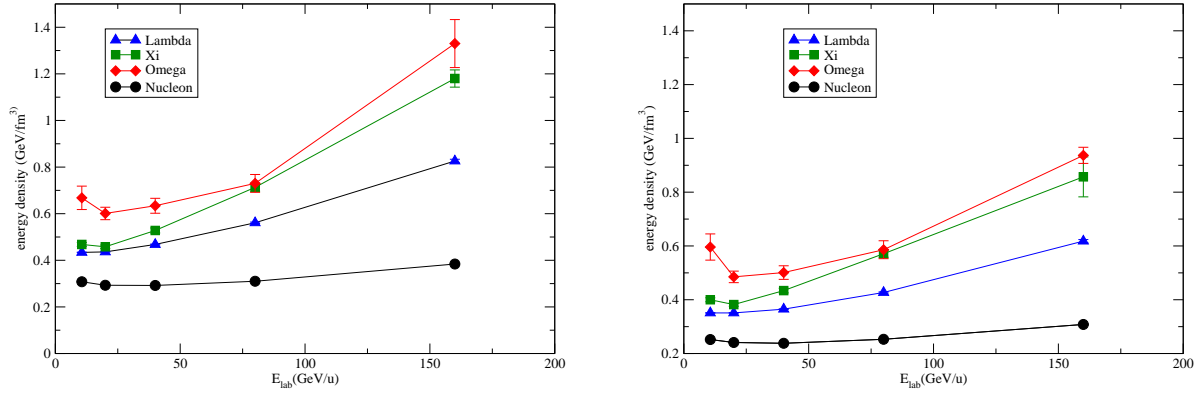


**Figure 7.** Average freeze-out energy density vs beam energy for final state baryons. The freeze-out energy-density is calculated at the average freeze-out time (left) and at the time when 80 percent of Nucleons, Lambda, Xi and Omega have ceased interacting (right).

the spread between the different baryonic states increase monotonously with increasing beam energy and approaches the values of the critical temperature and energy density of the QCD deconfinement transition at an incident beam energy of 160 GeV/nucleon. Our findings give rise to the speculation that for the  $\Omega$  this should be a universal value in the case of a hadronizing Quark-Gluon-Plasma.

## 7. Acknowledgments

This work was supported by the DOE under grant DE-FG02-05ER41367 and the CSC Scholarship program. Zhenglian Xie would like to thank Nankai University for giving the chance to do the research work in Duke University. Zhenglian Xie also thanks Prof. Berndt Mueller for helpful discussions and Duke University for the hospitality during her one year stay for the research work.

## References

- [1] Kolb E W and Turner M S 1990 *Front. Phys.* **69** 1–547
- [2] Collins J C and Perry M J 1975 *Phys. Rev. Lett.* **34** 1353
- [3] Shuryak E V 1980 *Phys. Rept.* **61** 71–158
- [4] Adcox K *et al.* (PHENIX) 2005 *Nucl. Phys.* **A757** 184–283 (*Preprint nucl-ex/0410003*)
- [5] Back B B *et al.* 2005 *Nucl. Phys.* **A757** 28–101 (*Preprint nucl-ex/0410022*)
- [6] Adams J *et al.* (STAR) 2005 *Nucl. Phys.* **A757** 102–183 (*Preprint nucl-ex/0501009*)
- [7] Arsene I *et al.* (BRAHMS) 2005 *Nucl. Phys.* **A757** 1–27 (*Preprint nucl-ex/0410020*)
- [8] Ludlam T 2005 *Nucl. Phys.* **A750** 9–29
- [9] Gyulassy M and McLerran L 2005 *Nucl. Phys.* **A750** 30–63 (*Preprint nucl-th/0405013*)
- [10] Harris J W and Muller B 1996 *Ann. Rev. Nucl. Part. Sci.* **46** 71–107 (*Preprint hep-ph/9602235*)
- [11] Bass S A, Gyulassy M, Stoecker H and Greiner W 1999 *J. Phys.* **G25** R1–R57 (*Preprint hep-ph/9810281*)
- [12] Rafelski J and Muller B 1982 *Phys. Rev. Lett.* **48** 1066
- [13] Koch P, Muller B and Rafelski J 1986 *Phys. Rept.* **142** 167–262

- [14] Koch P, Muller B, Stoecker H and Greiner W 1988 *Mod. Phys. Lett.* **A3** 737–742
- [15] Braun-Munzinger P, Stachel J, Wessels J P and Xu N 1995 *Phys. Lett.* **B344** 43–48 (*Preprint nucl-th/9410026*)
- [16] Letessier J, Tounsi A and Rafelski J 1996 *Phys. Lett.* **B389** 586–594
- [17] Vance S E and Gyulassy M 1999 *Phys. Rev. Lett.* **83** 1735–1738 (*Preprint nucl-th/9901009*)
- [18] Soff S *et al.* 1999 *Phys. Lett.* **B471** 89–96 (*Preprint nucl-th/9907026*)
- [19] Braun-Munzinger P, Heppel I and Stachel J 1999 *Phys. Lett.* **B465** 15–20 (*Preprint nucl-th/9903010*)
- [20] Rafelski J, Letessier J and Torrieri G 2001 *Phys. Rev.* **C64** 054907 (*Preprint nucl-th/0104042*)
- [21] Braun-Munzinger P, Magestro D, Redlich K and Stachel J 2001 *Phys. Lett.* **B518** 41–46 (*Preprint hep-ph/0105229*)
- [22] Andersen E *et al.* 1998 *Phys. Lett.* **B433** 209–216
- [23] Appelshauser H *et al.* (NA49) 1998 *Phys. Lett.* **B444** 523–530 (*Preprint nucl-ex/9810005*)
- [24] Bearden I G *et al.* (NA44) 1997 *Phys. Rev. Lett.* **78** 2080–2083
- [25] Adams J *et al.* (STAR) 2004 *Phys. Rev. Lett.* **92** 182301 (*Preprint nucl-ex/0307024*)
- [26] Abelev B I *et al.* (STAR) 2008 *Phys. Rev.* **C77** 044908 (*Preprint 0705.2511*)
- [27] van Hecke H, Sorge H and Xu N 1998 *Phys. Rev. Lett.* **81** 5764–5767 (*Preprint nucl-th/9804035*)
- [28] Dumitru A, Bass S A, Bleicher M, Stoecker H and Greiner W 1999 *Phys. Lett.* **B460** 411–416 (*Preprint nucl-th/9901046*)
- [29] Nonaka C and Bass S A 2007 *Phys. Rev.* **C75** 014902 (*Preprint nucl-th/0607018*)
- [30] Hirano T, Heinz U W, Kharzeev D, Lacey R and Nara Y 2008 *Phys. Rev.* **C77** 044909 (*Preprint 0710.5795*)
- [31] Bass S A *et al.* 1998 *Prog. Part. Nucl. Phys.* **41** 225–370 (*Preprint nucl-th/9803035*)
- [32] Bleicher M *et al.* 1999 *J. Phys.* **G25** 1859–1896 (*Preprint hep-ph/9909407*)